Theoretical calculation of the adiabatic electron affinities of the monosubstituted benzaldehyde derivatives

Par Pr. Zaki Safi

Theoretical calculation of the adiabatic electron affinities of the monosubstituted benzaldehyde derivatives

Zaki S. Safi[a*] and Nuha Wazzan[b]

Abstract

In the current study, several computational models were examined to calculate accurate adiabatic electron affinity (AEA) of twelve *m*- and *p*-monosubstituted benzaldehyde derivatives. The examined models are as follows: (i) composite high-level ab initio (G3B3, G4, CBS-Q, and CBS-QB3), (ii) Three hybrid DFT approaches (B3LYP, CAM-B3LYP, and wB97XD) with two basis

sets (6-31+G(d,p) and 6-311++G(2df,2p)) and (iii) single point calculation using fifteen DFT approaches with 6-311++G(2df,2p) at the B3LYP/6-31+G(d,p) geometry. Several statistical descriptors were computed to validate the calculated AEAs based on the available experimental results. Results revealed that G3B3 and CBS-QB3 are the most accurate result, while G4 and CBS-Q methods yield less accurate ones. Also, the wB97XD and CAM-B3LYP in combination with 6-311++G(2df,2p) able to calculate accurate AEAs. Low CPU time single point calculation strategy by using wb97 and wb97X approaches can compute AEAs value as accurately as G3B3 and CBS-QB3 methods. The AEAs of other several monosubstituted benzaldehydes were also predicted by using the wb97, wb97X, and wb97XD. The effect of the nature and position of substituents on the natural spin density and natural charge is also studied and discussed.

Keywords: *Adiabatic electron affinity (AEA), Composite high level ab initio methods (G3B3; CBS-QB3); Hybrid DFT approaches (wB97, wB97X, wB97XD, and CAM-B3LYP); substitution effect; Natural spin densities; SOMO; HOMO*

1. Introduction

Electron affinity, ionization potential, proton affinity and basicity are not only assessing in estimating the capability of atom or molecule to accept proton and donate electrons, but also play a crucial role in chemistry, environmental chemistry, proton transfer and electron-transfer

processes that occur in gas, liquid or solid phase [1-3]. Generally, the change in energy associated to the attachment of an electron with the chemical system is known as the electron affinity (EA). Adiabatic electron affinity (AEA) is directly related to the energy required to add an electron to an atom or a molecule. The stronger the attachment, the more energy is released. Unfortunately, experimental measurement and/or accurate theoretical calculation of EA are often not easy, and several techniques are experimentally available to measure electron affinity [4-6], such as low-energy electron transmission spectroscopy (ETS) [4], electron spin resonance (ESR) [5] and Fourier transform ion cyclotron resonance mass spectrometry (FT-ICR) [6]. On the other hand, many computational methods have been used to calculate the EAs of the chemical system [7, 8]. High-level *ab-initio* and post Hartree-Fock methods require very long CPU time and they are computationally cost, and they are able to compute accurate EAs for atoms and small molecules only, with an error of 1-3 kcal/mol. An alternative approach is to use the DFT method, which is one of the most powerful computational methods available for computing the EA, especially for medium and large molecule, with an estimated error of 4.6 kcal/mol (0.2 eV), compared to the experimental ones [9]. Electron affinities of uracil and some of its derivatives were calculated using DFT method [10], and a comparable EAs values with the experimental values were achieved. Fry et al [11] determined computationally the EAs of monosubstituted benzalacetophenones (Chalcones) using hybrid B3LYP approach with 6-31G(d) basis set. The EAs of some fluoro-*p*-benzoquinione derivatives were computed by using the G3(MP2)-RAD method, and well agreement with the experimental results was obtained [12]. The EAs of formamide and its methylation derivatives were determined by using different several computational methods such as DFT, ab initio HF and Moller-Plesset perturbation theory (MP) at 6-311++G(d,p) basis sets [13]. Cooper et al [14] determined the EAs values for six common explosives using different composite ab initio methods and some hybrid DFT methods, and they found that MP2 and B2PLYPD methods predicted EAs as accurately as CBS-QB3 approach. In comparison to the experimental data, the many-body Green's-function method predicted accurate ionization potential and electron affinity values [15]. The CCSD(T)/CBS//B3LYP/aug-cc-pVTZ and the G3 models were used to calculate accurate EAs in comparison to experimental results [8].

For this work, benzaldehyde and some of its derivatives have been chosen, which have several applications in chemistry, pharmacy and agriculture. One of the largest applications of the benzaldehyde in chemistry is in the production of certain polymeric materials. In addition, it can

be used in tanning and preserving materials, and as fungicide and insecticide. Recently, the proton affinities, gas-phase basicity, vertical ionization potential and vertical adiabatic ionization potential and adiabatic ionization potential have been calculated for eight benzaldehyde derivatives [2, 3]. The EAs of benzaldehyde and its derivatives have been experimentally estimated to range from 9.09-9.9 kcal/mol [16]. Pluharova et al [17] showed that the calculated EAs are sensitively basis sets dependent.

In this study, three main objectives will be considered to achieve. The first goal is to calculate the AEA for twelve monosubstituted benzaldehyde derivatives (Figure 1) by using three different computational strategies and the accuracy and the validation of the different strategies will be statistically approved based on the available experimental data. The second aim was undertaken to use the most accurate and economical strategy to calculate the AEAs of an additional seventeen benzaldehyde derivatives whose AEAs have not been determined theoretically and experimentally to the best of our knowledge. Finally, the nature of the substituted groups and their meta- or para- position are examined and discussed.

2. Calculation details

Three different computational strategies were used to calculate the AEAs of the twelve benzaldehyde derivatives. The first strategy is based on performing four composite high-level ab initio methods G4 [18], G3B3 [19], CBS-Q [20] and CBS-QB3[21]. Performing a full optimization processes of the neutral species and their anion radicals using three hybrid DFT methods (B3LYP [22], CAM-B3LYP [23] and wB97XD [24]) with 6-31+G(d,p) and 6-311++G(2df,2p) basis sets is the second strategy. Finally, the third strategy depends on carrying a single point calculation using several DFT approaches with 311++G(2df,2p) basis set at the B3LYP/6-31+G(d,p) geometry. The selected DFT functionals are as follows: B3LYP [22], B3PW91, CAM-B3LYP [23], BMK [25], B97D [26], TPSSTPSS [27], M11 [28], wB97 [29], wB97X [30], wB97XD [24], M05-2x [31], M06 [30], M06-L [32], M06-2X [33] and N12-NX [34]. For all strategies, frequency calculation was performed as usual to ensure that all structures are minima in the potential energy surface and also to extract the zero-point energy (ZPE). Gaussian 09 programs package [35] was performed to perform all computations.

The AEA without/with zero-point energies (ZPE) is calculated according to the following equations.

$$AEA = E^o - E^-$$ (1)

$$AEA_{(ZPVE)} = (E^o + ZPE) - (E^- + ZPE) \qquad (2)$$

where E^o and E^- are the optimized electronic energies of the neutral species and the corresponding anion radicals, respectively. For positive AEAs, the anion species is more stable than the neutral one and vice versa.
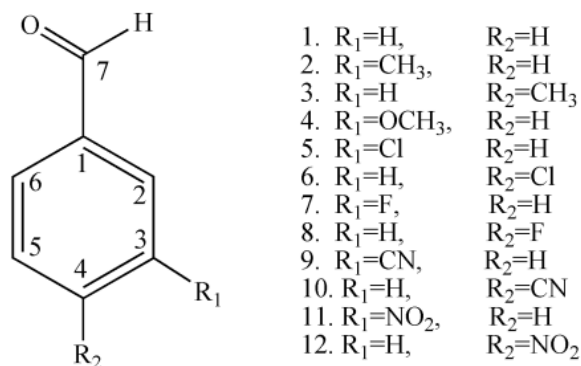

Figure 1. Chemical structure of the benzaldehyde derivatives.

3. Results and discussion

The zero-point energies and the total electronic energies of the investigated benzaldehyde derivatives are summarized in Tables S1-S6 of the supplementary materials. The AEAs values without zero-point energy as calculated by using all the suggested computational methods are available from authors upon request. Several statistical descriptors (see supplementary materials) were computed to validate the accuracy of the examined computational strategies in reference to the experimental values [36].

3.1. Analysis of composite high level *ab initio* and hybrid DFT methods

The twelve AEAs values of the investigated species as calculated using the suggested computational methods and the corresponding experimental results [36] are summarized in Table 1.The distributions of these values are also shown in Figure 2(a-c). In comparison with the experimental data, adequate agreements of the AEA values calculated using G_n and CBS methods can be clearly observed (Figure 2(a and b)). Additionally, the distributions of the combined AEA values of Gn (G4 and G3B3) and CBS (CBS-Q and CBS-QB3) series are also shown in Figure 2c, which show excellent consistencies with the experimental results.

The data presented in Table 1 demonstrate that the average AEA of G4 method are significantly higher than that of G3B3 method by 2.27 kcal/mol, which agrees with the previous studies [7]. Whereas, the average AEA of CBS-Q method are higher than that of CBS-QBS method by 0.94

kcal/mol. The average AEA values of G4, G3B3, CBS-Q and CBS-QB3 methods are higher than that of the experimental value by 2.81, 0.55, 2.78 and 1.84 kcal/mol, respectively.

Table 1. The AEA values of 12 benzaldehyde as calculated by using four composite ab initio methods (All values are in kcal mol^{-1}) and three hybrid DFT methods (B3LYP, CAM-B3LYP and wB97XD) in combination with two basis sets (BS1: 6-31+G(d,p) and BS2: 6-311++G(2df,2p)).

	EXPT [36].	G$_n$		CBS		B3LYP		CAM-B3LYP		wB97XD		Av1^a	Av2^b
		G4	G3B3	CBS-Q	CBS-QB3	BS1	BS2	BS1	BS2	BS1	BS2		
H	10.12	12.72	10.53	11.05	10.94	12.49	13.01	10.99	9.05	9.41	9.74	10.74	9.40
3-CH$_3$	9.41	12.8	10.27	9.428	10.97	12.1	12.57	10.52	8.76	8.93	9.41	10.62	9.09
4-CH$_3$	8.60	11.21	8.361	10.98	9.54	10.79	11.11	9.04	6.93	7.55	7.7	8.95	7.32
3-OCH$_3$	9.89	10.16	10.91	13.76	11.82	14.4	13.25	10.46	9.8	8.66	8.65	11.37	9.23
3-Cl	15.40	19.58	17.25	19.95	18.21	20.38	20.69	18.88	17.01	17.33	17.53	17.73	17.27
4-Cl	15.20	17.78	15.48	18.53	16.74	18.92	19.22	17.57	15.68	16.04	16.25	16.11	15.97
3-F	15.40	17.78	15.19	17.11	16.07	18.5	18.53	17.23	15.07	15.39	15.33	15.63	15.20
4-F	11.21	13.08	10.52	13.36	11.78	14.44	14.28	12.99	10.34	11.14	10.82	11.15	10.58
3-CN	23.33	27.78	25.29	21.96	26.45	29.01	29.4	26.89	25.26	25.41	25.81	25.87	25.54
4-CN	28.16	31.89	29.71	35.87	30.63	34.51	34.77	32.55	31.37	31.17	31.42	30.17	31.40
3-NO$_2$	32.98	36.01	32.86	40.5	35.71	41.56	40.72	39.42	36.65	37.02	35.86	34.29	36.26
4-NO$_2$	39.00	41.62	38.85	39.52	41.87	48.34	47.57	45.78	43.63	43.49	42.41	40.36	43.02
average	**18.14**	**21.03**	**18.77**	**21.00**	**20.06**	**22.95**	**22.93**	**21.03**	**19.13**	**19.30**	**19.24**	**19.41**	**19.19**

^{a} Av1 corresponds to the average AEA values of the G3B3 and CBS-QB3 methods
^{b} Av2 corresponds to the average AEA values of the wB97XD and CAM-B3LYP methods in combination with BS2.

The AEAs calculated using the three hybrid DFT approaches: B3LYP, CAM-B3LYP and wB97XD, in combination with the 6-31+G(d,p) and 6-311++G(2df,2p) basis sets are also presented in Table 1 and their distributions are also depicted in Figure 2(d-e), together with the experimental results. Generally, very good matching is observed between the experimental EA values and the AEA as calculated by using the DFT approaches.

For 6-31+G(d,p) basis set, the average value of AEA as calculated by using B3LYP and CAM-B3LYP approaches are 3.66 and 1.73 kcal/mol, respectively, much higher than that calculated by wB97XD approach. Interestingly, for 6-311++G(2df,2p) basis sets, the difference between the average AEA value calculated by B3LYP approach is 3.68 kcal/mol much higher than wB97XD approach, while the average AEA value in the case of CAM-B3LYP functional becomes almost equal to that of wB97XD functional.
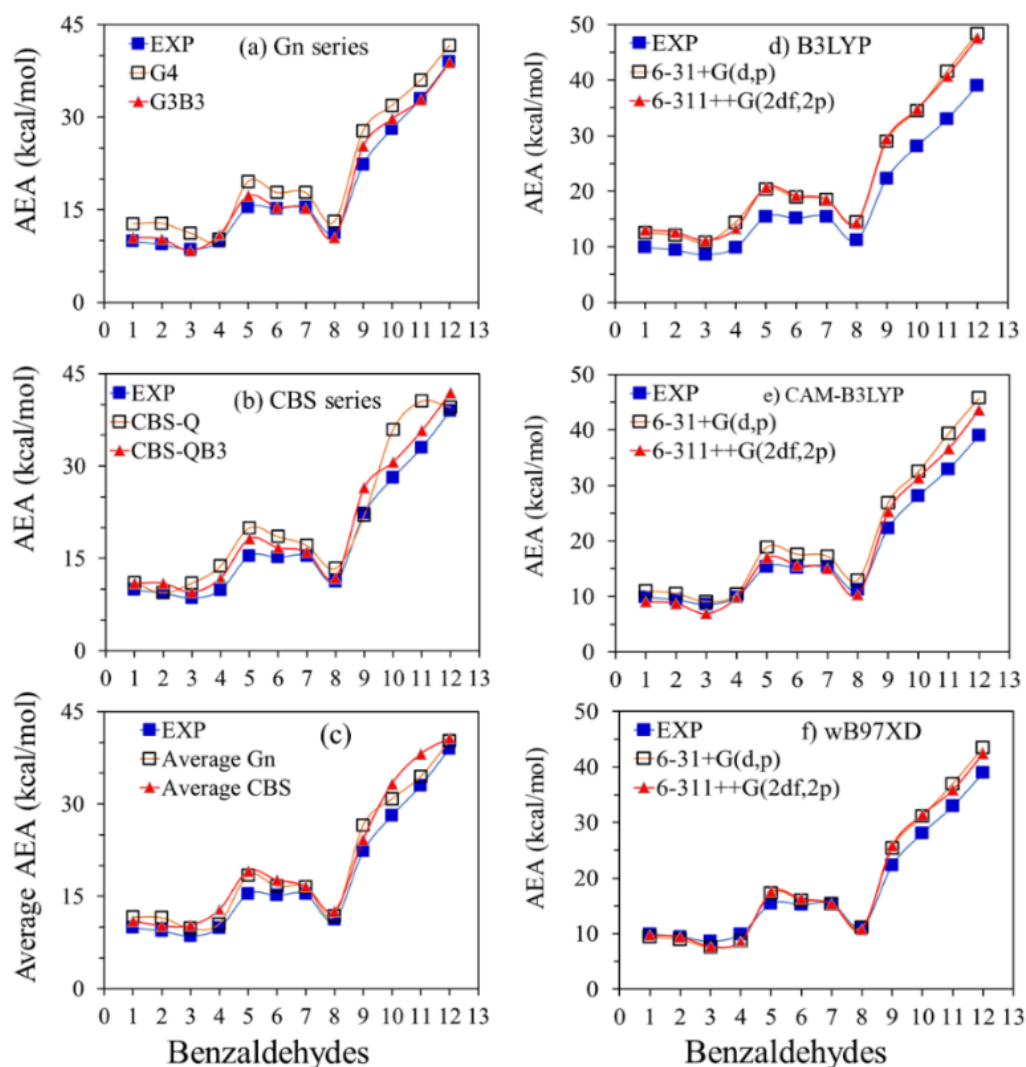
Figure 2. The 12 AEAs distributions as obtained by (a) G_n methods (b) CBS methods, (c) the averages of G_n and CBS methods, (d) B3LYP (e) CAM-B3LYP and (f) wB97XD methods. In all panels, available experimental AEA values are shown by filled blue circles [36]. All values are in kcal/mol.

The results show that the average AEAs as calculated by using wB97XD approach with 6-31+G(d,p) and 6-311++(2df,2p) basis sets are highly matching the experimental results with a difference of 1.07 and 1.02 kcal/mol. For B3LYP approach, the average AEA value is ~ 4.7 kcal/mol higher than that of the experimental AEA value, regardless of the elected basis sets. For

the CAM-B3LYP functional, the average AEA values obtained by using 6-31+G(d,p) and 6-311++(2df,2p) bases sets are 2.81 and 0.91 kcal/mol, respectively, higher than the experimental results data.

However, G3B3 and CBS-QB3 methods as well as the wB97XD and CAM-B3LYP approaches in combination with 6-311++G(2df,2p) basis set can compute very good AEA values, but they require a very long CPU time and they are not advisable to compute the AEA for larger compounds. Unfortunately, optimization of the large chemical compounds using the 6-311++G(2df,2p) basis sets is computationally cost compared to 6-31+G(d,p) basis set. So that, it is very important to find an alternative pathway to compute accurate AEA values with low CPU time. B3LYP method is, in the mixed functional, relatively simple, and geometrical calculations speed is fast, and it has low dependence on the integration grid point. However, B3LYP has succeeded in many applications, such as geometrical structure [2, 3, 37, 38], but unfortunately, it has been failed in the computation of the ionization potential and electron affinity, which it only computes 70-75% of the actual values [3]. It was suggested that B3LYP could be modified by remote mixing density functionals like wB97X or wB97XD [39, 40], which is fast and low CPU time-consuming. Alternatively, to achieve accurate AEAs value with low computation cost, single point calculation using fifteen different DFT approaches in combination with the 6-311++G(2df,2p) bases set at the B3LYP/6-31+G(d,p) geometries of both neutral and its radical anions is used. The results obtained are summarized in Table 2. Inspection of Table 2 shows that the average AEA calculated by the BMK, wb97, wb97X and wb97XD are the closest ones to the experimental results. It is found that the average AEA values of the mentioned DFT approaches are higher than the experimental values by 1.11, 1.16, 1.28 and 1.46 kcal/mol. Whereas, the poorest results are reported by B3LYP, B3PW91 and B97D. The average AEA value calculated by approaches are much higher than that of the experimental value by 4.89, 4.88 and 4.53 kcal/mol, respectively.

Furthermore, correlation of the different computational methods examined here shows a linear relationships correlation with R^2 very close to unity (Figure S1 of the supplementary materials). For example, the results of AEAs of CBS-QB3, CAM-B3LYP/6-311++G(2df,2p) and wB97XD/6-311++G(2df,2p) are linearly correlated with those of G3B3 with $R^2 = 0.9978, 0.9965$ and 0.9972, respectively. Additionally, the average AEA values of G3B3 and CBS-QB3 are also linearly

correlated with those of the combination of CAM-B3LYP and wB97XD with 6-311++G(2df,2p) with $R^2 = 0.9983$.

Table 2. The AEA values of monosubstituted benzaldehydes as calculated by using single-point calculations of 14 DFT functionals based on the B3LYP/6-31+G(d,p) geometry (All values are in kcal mol^{-1}).

	1	2	3	4	5	6	7	8	9	10	11	12	13	14	15
H	9.84	9.89	9.96	12.92	13.11	12.71	8.85	11.86	11.44	12.23	10.88	10.36	10.36	12.26	11.63
3-CH$_3$	9.55	9.57	9.59	12.67	12.79	12.46	8.56	11.54	11.24	12.17	10.77	9.99	9.99	12.11	11.31
4-CH$_3$	7.90	7.94	8.03	11.21	11.39	11.25	6.93	10.04	9.46	10.75	9.06	8.69	8.69	10.94	9.69
3-OCH$_3$	12.01	11.92	11.79	14.79	14.91	14.61	10.81	14.08	13.56	14.51	13.02	12.42	12.42	14.28	13.61
3-Cl	17.41	17.57	17.68	20.73	20.78	20.32	17.15	19.71	19.44	19.84	18.76	18.00	18.00	20.11	19.40
4-Cl	16.20	16.37	16.45	19.29	19.33	18.83	15.64	18.47	17.89	18.40	17.29	16.41	16.41	18.60	18.10
3-F	15.84	15.69	15.54	18.57	18.50	17.85	14.56	18.03	17.56	17.69	16.57	15.42	15.42	17.64	17.50
4-F	11.21	11.13	11.05	14.29	14.12	13.84	9.79	13.52	12.76	13.17	11.81	10.78	10.78	13.52	13.03
3-CN	25.23	25.45	25.89	29.49	29.93	29.78	25.52	27.60	27.73	29.03	26.67	27.77	27.77	29.35	27.57
4-CN	31.11	31.29	31.65	34.90	35.37	34.83	31.26	33.44	33.70	34.39	32.69	33.19	33.19	34.50	33.21
3-NO$_2$	35.05	35.43	35.97	40.79	40.01	40.00	38.02	37.71	38.74	39.79	37.07	38.00	38.00	40.02	38.67
4-NO$_2$	41.19	41.74	42.60	47.62	46.98	46.54	44.93	44.09	45.66	46.48	44.07	44.87	44.87	46.62	45.18
average	19.38	19.50	19.68	23.11	23.10	22.75	19.34	21.67	21.60	22.37	20.72	20.49	20.49	22.50	21.58
ΔAEA*	1.16	1.28	1.46	4.89	4.88	4.53	1.11	3.45	3.38	4.15	2.50	2.27	2.27	4.28	3.35

1: wb97, 2: wB97X, 3: wB97XD, 4: B3LYP, 5, B3PW91, 6: B97D, 7: BMK, 8: M11 , 9: M05-2X, 10: M06, 11: M06-2X, 12: M06-L, 13: N12-SX, 14: TPSSTPSS, 15: CAM-B3LYP.

$\Delta AEA = AEA_{calc} - EA_{exp}$

3.2. Statistical analysis

The accuracy of the different computational methods, which were applied to calculate the AEAs of the twelve benzaldehyde derivatives can be well examined by computing several statistical descriptors such as MAX, MAD, MD and RMSE. Full details about these statistical descriptors and the equations than can be used to calculate them are given in the supplementary materials. The most relevant statistical descriptors are displayed in Table 3. The graphical representation of RMSE values is shown in Figure 3. Furthermore, possible linear correlations between the calculated AEAs using the different computational methods and the experimental ones are also examined. The values of R^2, slopes, and intercepts of all the expected correlation are also gathered in Table 3. In all cases, excellent linear correlations between the 12 AEAs calculated by the different computational methods and the experimental ones are obtained with R^2 very close to unity (See Figure S2 of supplementary materials).

For the first strategy, inspection of Table 3 and Figure S3 indicates that among the Gn and CBS series, the lowest **RMSE** values (the most accurate method) of 1.22 kcal/mol is found for the G3B3 method, whereas, the largest one (least accurate) is found for CBS-Q method. Therefore, the accuracy of the different G_n and CBS series can be arranged as follows: G3B3 > CBS-QB3 > G4 > CBS-Q.

For the second strategy, the data given in Table 3 and shown in Figure S3 suggest that the smallest RMSE (most accurate) is computed by wB97XD/6-311++G(2df,2p) level of theory, while the highest one (least accurate) is reported for B3LYP/6-11+G(d,p) level of the theory. It is also found that the RMSE value reported for CAM-B3LYP/6-311++G(2df,2p) is slightly higher than that reported for wB97XD/6-311++G(2df,2p) by ~ 0.20 kcal/mol. Based on the RMSE values, the accuracy of the three hybrid DFT approaches can be ranked as follows: wB97XD/6-311++G(2df,2p) > CAM-B3LYP/6-311++G(2df,2p) > wB97XD/6-31+G(d,p) > CAM-B3LYP/6-31+G(d,p) > B3LYP/6-311++G(2df,2p) > B3LYP/6-31+G(d,p). The MAX values are 3.00, 3.18, and 3.60 kcal/mol, respectively. The results reveal that B3LYP approach is not a good choice to compute the AEAs, regardless of the basis set examined, while the wB97XD and CAM-B3LYP are good choices, especially with 6-311++G(2df,2p) basis set, and they able to compute AEA as accurate as the Gn and CBS series.

For DFT/6-311++G(2df,2p)//B3LYP/6-31+G(d,p) approaches, based on RMSE values the wb97 is the most accurate approaches, while the B3PW91 and B3LYP are the least accurate ones. Indeed, the computed RMSE values for wb97, wb97x, and wb97XD approaches are 1.76, 1.92, and 2.20 kcal/mol, while those that are reported for B3LYP and B3PW91 approaches are 5.34 and 5.38 kcal/mol. Additionally, we find out that BMK, M06-2X, M06-L, and N12-SX methods give a moderate accuracy with RMSE values of 2.78, 3.06, 3.30, and 3.41 kcal/mol. Based on the data listed in Table 3 and shown in Figure S3, the fifteen DFT approaches can be ranked, according to their accuracy (from highest to lowest), as follows: wB97 > wB97X > wB97XD > BMK > M06-2X > M06-L > N12-SX > M11 > CAM-B3LYP > M05-2X > M06 > TPSSTPSS > B97D > B3PW91 > B3LYP. It is important to mention that, however the CPU time required to compute the AEA using the wb97 and wb97X with 6-311++G(2df,2p) at the B3LYP/6-31+G(d,p) geometry is much shorter than that of the hybrid DFT with 6-311+G(2df,2p) basis set, the accuracy of the AEA value computed by the former is higher than that of the later.

Table 3. Statistical correlations between the 12 AEAs calculated by the proposed computational methods with the corresponding experimental values (All results are in kcal/mol). The Table is sorted by RMSE column.

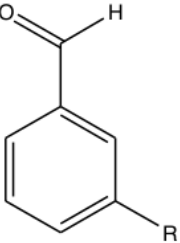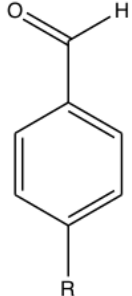|	MAX	MAD	MD	RMSE	R^2	Slope	intercept
Gn series							
G3B3	2.99	0.87	0.63	**1.21**	0.989	0.980	-0.330
G4	5.48	2.90	2.90	**3.15**	0.987	0.950	-1.850
CBS seies							
CBS-QB3	4.15	1.93	1.93	**2.20**	0.994	0.930	-0.500
CBS-Q	7.76	2.92	2.87	**3.85**	0.949	0.880	-0.280
Full optimization using hybrid DFT							
wB97X (BS2)	3.51	1.59	1.13	**2.07**	0.860	1.530	0.860
CAM-B3LYP (BS2)	4.63	1.76	1.01	**2.27**	0.830	2.190	0.830
wB97XD (BS1)	4.49	1.73	1.18	**2.29**	0.840	1.960	0.840
CAM-B3LYP (BS1)	6.78	2.91	2.91	**3.60**	0.830	0.770	0.830
B3LYP (BS2)	8.57	4.81	4.81	**5.23**	0.830	-0.920	0.830
B3LYP (BS1)	9.35	4.84	4.84	**5.36**	0.810	-0.560	0.810
DFT/6-311++G(2df,2p)//B3LYP/6-31+G(d,p) approach							
wb97	3.00	1.41	1.24	**1.76**	0.993	0.913	0.436
wb97x	3.18	1.53	1.37	**1.92**	0.994	0.900	0.594
wb97xd	3.60	1.70	1.55	**2.20**	0.993	0.878	0.851
BMK	5.93	2.21	1.20	**2.78**	0.995	0.802	2.633
M06-2x	5.07	2.59	2.59	**3.06**	0.993	0.872	0.070
M06-L	5.87	2.43	2.36	**3.30**	0.990	0.822	1.288
N12-SX	6.72	2.48	2.46	**3.41**	0.995	0.811	1.425
M11	5.33	3.54	3.54	**3.80**	0.994	0.895	-1.255
Cam-B3LYP	6.19	3.44	3.44	**3.84**	0.995	0.861	-0.430
M05-2x	6.66	3.46	3.46	**3.96**	0.995	0.845	-0.118
M06	7.48	4.24	4.24	**4.69**	0.993	0.841	-0.672
TPSSTPSS	7.63	4.36	4.36	**4.82**	0.993	0.837	-0.701
B97D	7.54	4.61	4.61	**5.02**	0.992	0.845	-1.086
B3PW91	7.99	4.97	4.97	**5.34**	0.993	0.846	-1.414
B3LYP	8.62	4.97	4.97	**5.38**	0.995	0.834	-1.140

According to the above discussion, we can safely conclude that using the wB97 and/or wB97x with 6-311++G(2df,2p) basis at the B3LYP/6-31+G(d,p) geometry able to reproduce AEA as accurate as those computed by G3B3, CBS-QB3 and they are a good choice in terms of CPU time and accuracy.

3.3.   Prediction of the AEAs of some substituted benzaldehyde.

According to the results obtained the AEAs of seventeen monobenzaldehyde derivatives were calculated using the wb97, wb97X, and wB97XD with 6-311++G(2df,2p) bases set at the

B3LYP/6-31+(d,p) geometry. The results are gathered in Table 4 and full set of data are collected in Table S6 of the supplementary materials. To our best knowledge, the AEAs of most of the chosen derivatives were not reported in the literature.

Table 4. The AEA values of 17 m- and p-monosubstituted benzaldehyde derivatives as calculated by using single point calculations of wb97, wb97X, wB97XD, and MBK hybrid DFT functionals with 6-311++G(2df,2p) bases set based on the B3LYP/6-31+(d,p) geometry (All values are in kcal mol^{-1}).

	Species	Method			Average
		wb97	wb97x	wb97XD	
	3-CHO	21.36	21.84	22.77	21.99
	3-OH	11.58	11.46	11.27	11.44
	3-COOH	19.36	19.64	20.33	19.78
	3-COOCH$_3$	15.78	15.98	16.50	16.09
	3-NH$_2$	8.32	8.20	8.00	8.17
	3-N(CH$_3$)$_2$	7.63	7.47	7.23	7.45
	3-ph	14.15	14.44	15.10	14.56
	3-OCOCH$_3$	21.60	21.51	21.43	21.51
	4-CHO	31.80	32.16	32.82	32.26
	4-OH	21.36	21.84	22.77	21.99
	4-COOH	28.27	28.42	28.82	28.50
	4-COOCH$_3$	25.99	26.20	26.66	26.28
	4-NH$_2$	2.17	2.05	1.89	2.04
	4-N(CH$_3$)$_2$	4.04	3.93	3.72	3.89
	4-ph	20.03	20.16	20.73	20.31
	4-OCH$_3$	5.49	5.54	5.51	5.51
	4- OCOCH$_3$	19.01	18.98	18.95	18.98

The results obtained show that the predicted average AEA values of the examined derivatives vary from 7.45 to 32.26 kcal/mol and these values are well compared with those of the twelve known benzaldehydes, supporting the selected methodology.

3.4.   Analysis of the substituent effect on the calculated AEA values.

The changes in the AEA values of the benzaldehyde derivatives as calculated by using the wB97/6-311++G(2df,2p)//B3LYP/6-31+G(d,p) approach, due to the substitution of the different groups at m- and p-position (ΔAEA) is given by the following equation.

$$\Delta AEA = AEA_{(benzaldehyde\ derivative)} - AEA_{(parent\ benzaldehyde)} \qquad (3)$$

The ΔAEA is graphically shown in Figure 3. It is indicated that substitution of electron-withdrawing groups (EWGs) increases AEA values, and the reverse is true in the case of electron-donating groups (EDG). Actually, the ΔAEA are negative in the case of EDGs, with the exception of m-OCH$_3$, and they are positive for all EWGs, regardless of their position. It is found the AEAs of the p-NO$_2$ and m-NO$_2$ derivatives are the largest ones, with ΔAEA of 31.35 and 25.21 kcal/mol. Whereas, the p-NH$_2$ and p-N(CH$_3$)$_2$ derivatives have the smallest AEAs values among all the investigated species. Interestingly, the results also show, except of -F, -Cl, and -OCOCH$_3$ groups, that substitution of the EDGs and/or EWGs at the para position results in larger ΔAEA values compared to that at m-position (Figure 3). It is also found that the AEA of m-F is 4.63 kcal/mol higher than that of the p-F derivative. Additionally, the substitution effect of -OH group at meta position is neglected compared to that at para position. Indeed, our results show that the AEA of m-OH derivative is 9.78 kcal/mol lower than that of the p-OH derivatives.
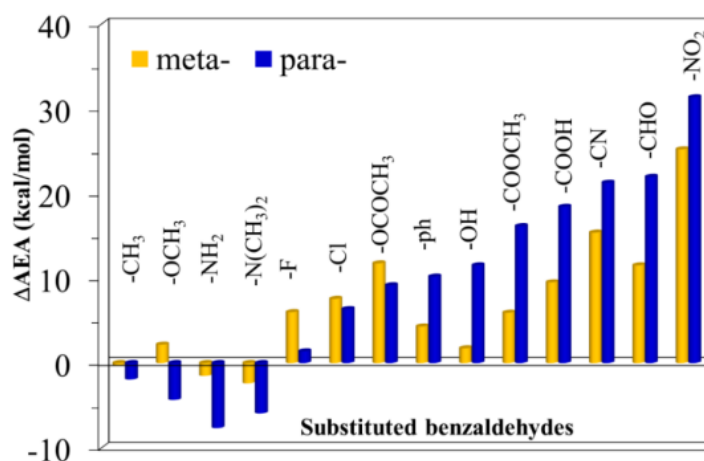

Figure 3. Graphical representation of the change in AEA of the m- and p-monosubstituted benzaldehyde with respect to the AEA of the parent benzaldehyde as computed using the wb97/6-311++G(2df,2p//B3LYP-6-31+G(d,p) level of theory in the gas phase. All values are in kcal/mol.

These results can be approved by considering the change in the natural spin densities and the natural charges. The natural charges and the corresponding natural spin densities were used to explain the changing pattern in the AEA of the m- and p-monosubstituted benzaldehyde at m- and p- position using the Natural Bond Orbital Analysis (NBO). The numerical values of the natural

spin densities and the natural charges of $m\text{-}NO_2$, $p\text{-}NO_2$, $m\text{-}N(CH_3)_2$ and $p\text{-}N(CH_3)_2$ derivatives are shown in Figure 4a. Whereas, the distribution of the spin densities and the singly occupied molecular orbitals (SOMO) for the anions for the same derivatives are also shown in Figure 4 (b and c). For the sake of comparison, the electron distribution of the HOMO surfaces of the corresponding neutral species are also show in Figure 4d.

It is well known that EWGs can decrease the electron density of a conjugated pi system, while the EDG can increase this conjugation. Additionally, EDGs can donate or release electrons and EWGs can withdraw electrons. In order to simplify our discussion, we will only follow the changes in the natural spin densities and natural charges of the carbon and atoms of the aldehyde group. It can be clearly observed that the substituent groups have different effects on the spin densities and the natural charges according to the type of the EDGs or EWGs and their replacing. For example, the substitution of NO_2 group (EWG) decreases the natural spin densities of the C and O atoms. Whereas, a reverse effect is observed in the case of the natural charges. Importantly, and in consistence with the calculated AEAs, substitution of NO_2 group at p- position has a higher effect than that at the *meta* position and the reverse effect is true in the case of the EDGs. That is to say, EWGs and/or EDGs decrease and/or increase the natural spin densities and increase and/or decrease the natural charges of the adjacent carbon atoms to the substitution position. The degree of the substitution effects greatly depends on the substitution position (meta or para). These effects can also be observed by monitoring the surfaces of the natural spin densities (Figure 4b).

Monitoring of Figure 4(b-d) shows that there are different effects on the natural atomic charges, natural spin densities of the adjacent carbon atoms to the substituted groups, as well as the carbonyl groups. It is also observed, upon anion formation, that the distribution of the electron densities of the SOMO, which occupies the incoming electrons, of the anions is completely different compared to the electron distribution of the HOMO of the corresponding neutral ones. Inspection of Figure 4c shows that the SOMO is located on the whole moiety of the anions, indicating that the incoming electron is the delocalization of the incoming electrons.
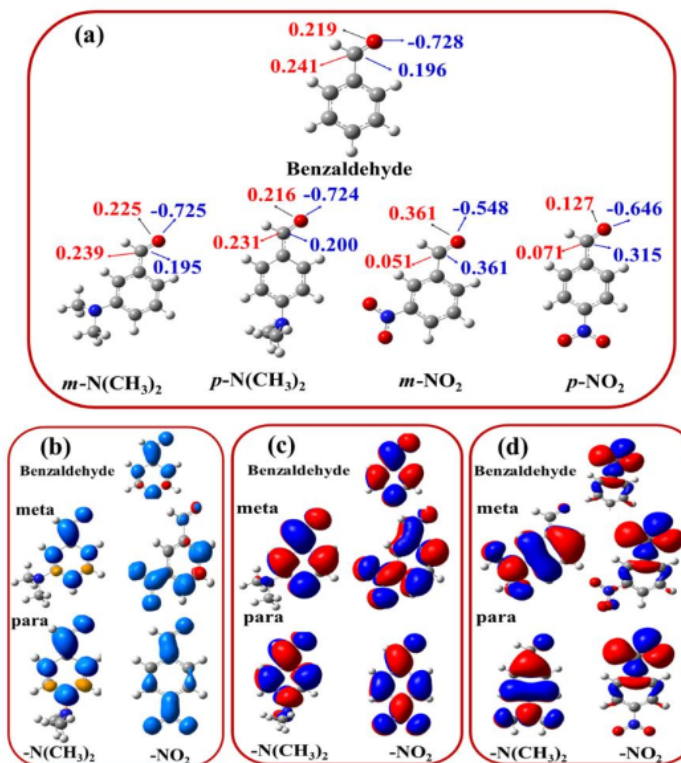
Figure 4. (a) Natural charges and the natural spin densities of some *m*- and *p*-monosubstituted benzaldehydes anions (benzaldehyde, --N(CH$_3$)$_2$ and NO$_2$) (Natural spin density in red and Natural charges in blue), (b) spin densities surfaces, (c) singly occupied molecular orbitals (SOMO) of radical anions and (d) highest occupied molecular orbital surfaces of the neutral species of some *m*- and *p*-monosubstituted benzaldehydes anions. The HOMO, SOMO, the natural spin densities, and the natural charges of the anions species are computed using the B3LYP/6-31+G(d,p) level of theory.

3.5. Influence of attaching excess electrons on the geometrical structure

Significant structural changes have occurred in the geometrical structures (bond lengths and bond angles) in radical anions compared to the neutral species. The change in the geometrical structures of the bonds C1-C7 and C7=O bond lengths and the angle C1-C7=O for the neutral species and their radical anions at B3LYP/6-31+G(d,p) are discussed. The most relevant geometrical structure parameters are listed in Table 5.

Table 5. The significant structural parameters (the bonds C1-C7, C7=O, and the angle C1-C7=O) of neutral and anionic states optimized of monosubstituted benzaldehyde derivatives at B3LYP/631+G(d,p) level of theory.

	neutral			anion		
	C1-C7	C7=O	C1-C7=O	C1-C7	C7=O	C1-C7=O
H	1.481	1.219	124.9	1.428	1.271	126.7
3-CH$_3$	1.480	1.219	125.0	1.429	1.269	126.8
3-NH$_2$	1.481	1.218	125.1	1.429	1.271	126.8
3-OCH$_3$	1.482	1.218	124.9	1.428	1.270	126.6
3-Cl	1.484	1.217	124.6	1.428	1.268	126.4
3-F	1.484	1.217	124.6	**1.428**	1.269	126.5
3-CN	1.486	1.216	124.3	1.435	1.258	126.2
3-NO$_2$	1.486	1.216	124.2	**1.461**	**1.233**	126.2
3-CHO	1.484	1.217	124.5	1.451	1.244	**127.3**
3-OH	1.483	1.218	124.8	1.429	1.270	126.6
3-COOH	1.484	1.218	124.5	1.444	1.249	126.3
3-COOCH$_3$	1.483	1.217	124.9	1.438	1.255	127.5
3-N(CH$_3$)$_2$	1.481	1.219	125.1	1.429	1.271	126.6
3-ph	1.481	1.218	124.9	1.440	1.255	126.4
3-OCOCH$_3$	1.484	1.217	124.6	1.429	1.266	126.4
4-CH$_3$	1.478	1.220	125.0	1.428	1.271	126.8
4-NH$_2$	1.469	1.223	125.4	1.428	1.272	126.6
4-OCH$_3$	1.473	1.221	125.2	1.428	1.270	126.6
4-Cl	1.480	1.218	124.7	1.428	1.268	126.5
4-F	1.479	1.219	124.8	1.428	**1.272**	126.4
4-CN	1.485	1.217	124.4	1.431	1.258	126.8
4-NO$_2$	1.487	1.216	124.2	1.443	1.243	126.9
4-CHO	1.485	1.217	124.5	1.435	1.252	127.0
4-OH	1.474	1.221	125.1	1.428	1.273	126.5
4-COOH	1.485	1.217	124.6	1.434	1.254	127.0
4-COOCH$_3$	1.484	1.218	124.7	1.433	1.255	127.0
4-N(CH$_3$)$_2$	1.466	1.224	125.5	1.428	1.269	**126.7**
4-ph	1.477	1.220	124.9	1.433	1.255	127.0
4- OCOCH$_3$	1.481	1.218	124.7	1.428	1.267	126.4
average	**1.481**	**1.218**	**124.8**	**1.433**	**1.262**	**126.7**
Change				-0.048	0.044	1.9

Inspection of Table 5 shows that the bond C1-C7 is decremented, the bond C7=O is incremented, and the angle C1-C7=O is opened. The average decrement of bond C1-C7 is 0.048 Å and the average increment of bond C7=O is 0.044 Å. The angle C1-C7=O is opened by 1.9°. Upon anion formation, the decrement in the bond C1-C7 is changed from 0.025-0.056 Å, the increment in the bond C7=O is ranged from $0.017 - 0.053$ Å, and angle C1-C7=O is opened is the range of 1.189

to 2.774°. The maximum decrement in the bond C1-C7 of 0.056 Å is reported for 3-F and 3-Cl derivatives, while the minimum decrement in the bond C1-C7 of 0.025 Å is reported for 3-NO$_2$ derivatives. The maximum increment in the bond C7=O of 0.054 Å is found for 4-F derivative and the lowest increment is found in the case of 3-NO$_2$ derivative. For the angle C1-C7=O, the minimum deviation of 1.2° is found for the 4-N(CH$_3$)$_2$ and 4-NH$_2$ derivatives, while the maximum deviation of 2.5° is reported for 3-CHO derivative.

Conclusions

- In the current study, the adiabatic electron affinities (AEAs) of the 12 *m*- and *p*-monosubstituted benzaldehyde were calculated using 4 different composite high-level *ab* methods (G3B3, G4, CBS-Q, and CBS-Q) and three hybrid DFT methods (B3LYP, CAM-B3LYP and wB97XD) with two bases sets (6-31+G(d,p) and 6-311++G(2df,2p).

- Among the high-level *ab initio* methods, the AEA calculated by G3B3 and CBS-QB3 methods are in excellent agreement with the experimental results, and they are good choices for computing the AEA, while the accuracy of the G4 and CBS-Q methods are lower than that of G3B3 and G4 and they are not good choices to calculate the AEA.

- Using the hybrid wB97XD and CAM-B3LYP functional with the 6-311++G(2df,2p) are also a good choice computation model to compute the AEA, but the 6-311++G(2df,2p) is highly CPU cost, especially for a larger system.

- The computation of the AEA by performing a single point calculation using the wB97, wB97X, and wB97XD functionals with 6-311++G(2df,2p) at the B3LYP/6-31+G(d,p) geometry can be used as alternative and cheaper computational to compute accurate AEA values.

- For the first time, the AEA of another 17 benzaldehyde derivatives were computed using the wB97, wB97X, and wB97XD functionals with 6-311++G(2df,2p) at the B3LYP/6-31+G(d,p) geometry. The AEAs of these derivatives are reasonable in comparison with the AEA of the known derivatives.

- All AEAs of the monosubstituted benzaldehyde derivatives are positive in the gas phase with all methods, indicating that all radical anions are stable with respect to electron attachment adiabatically and vertically in the gas phase.

- Our results showed that when the substituent is EDG, the predicted AEA is smaller than that of the parent benzaldehyde, while for the EWG, the AEA is higher than that of the

parent benzaldehyde. The greatest effect of EWG is observed in case of NO_2 group in both positions, while the largest effect of the EDG is observed for p-NH_2 derivative. In most case, substitution at *para-* position has a greater effect than that at *meta-* position.[7] Moreover, for the EWG, the natural spin densities of the C and O of the aldehyde group are smaller than those in the unsubstituted benzaldehyde, while the reverse effect is true in case of EDGs.[8]
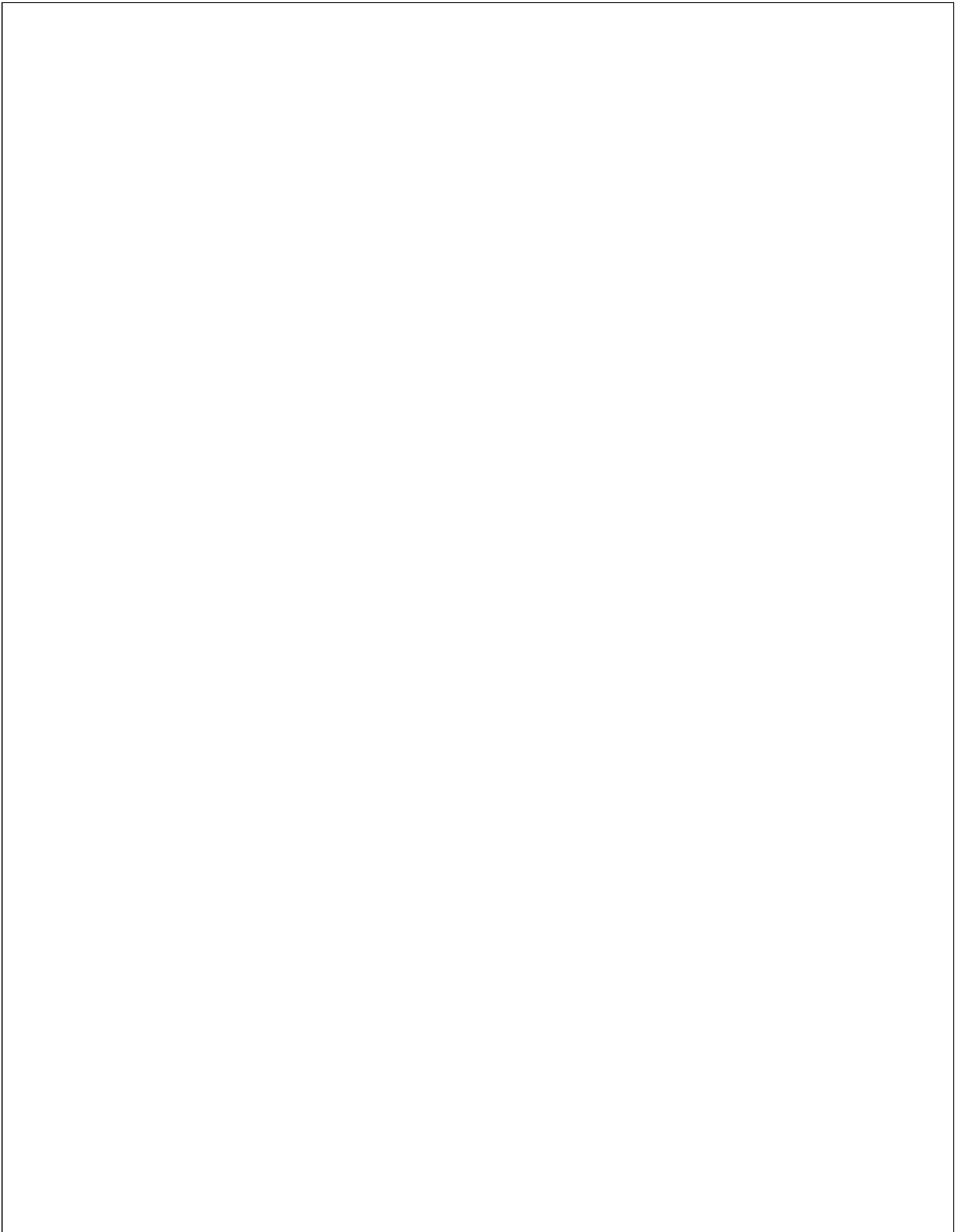
- The decrement of bond length of C1-C7 and the increment of bond length of C7=O and the opening of the bong angle C1-C7=O indicate that the structures of anionic states of[8] monosubstituted benzaldehydes have larger changes when comparing with the neutral state.

References

1. Safi, Z.S. and S. Omar, *Proton affinity and molecular basicity of m-and p-substituted benzamides in gas phase and in solution: A theoretical study.* Chemical Physics Letters, 2014. **610**: p. 321-330.
2. Safi, Z.S. and N. Wazzan, *Benchmark calculations of proton affinity and gas-phase basicity using multilevel (G4 and G3B3), B3LYP and MP2 computational methods of para-substituted benzaldehyde compounds.* Journal of computational chemistry, 2021. **42**(16): p. 1106-1117.
3. Safi, Z.S., N. Wazzan, and H. Aqel, *Calculation of vertical and adiabatic ionization potentials for some benzaldehydes using hybrid DFT, multilevel G3B3 and MP2 methods.* Chemical Physics Letters, 2022. **791**: p. 139349.
4. Modelli, A., et al., *Low-energy electron capture in group 14 methyl chlorides and tetrachlorides: Electron transmission and dissociative electron attachment spectra and MS-Xα calculations.* The Journal of chemical physics, 1998. **108**(21): p. 9004-9015.
5. Symons, M.C. and R.L. Petersen, *The relative electron affinities of the α and β chains of oxyhaemoglobin as a function of pH and added inositol hexaphosphate: An electron spin resonance study.* Biochimica et Biophysica Acta (BBA)-Protein Structure, 1978. **537**(1): p. 70-76.
6. Marshall, A.G., *Fourier transform ion cyclotron resonance mass spectrometry.* Accounts of chemical research, 1985. **18**(10): p. 316-322.
7. Yang, Y., et al., *Theoretical study on adiabatic electron affinity of fatty acids.* New Journal of Chemistry, 2021. **45**(36): p. 16892-16905.
8. Miller, T.M., et al., *Thermal Electron Attachment to Pyruvic Acid, Thermal Detachment from the Parent Anion, and the Electron Affinity of Pyruvic Acid.* The Journal of Physical Chemistry A, 2022.
9. Rienstra-Kiracofe, J.C., et al., *Atomic and molecular electron affinities: photoelectron experiments and theoretical computations.* Chemical reviews, 2002. **102**(1): p. 231-282.
10. Li, X., L. Sanche, and M.D. Sevilla, *Dehalogenation of 5-halouracils after low energy electron attachment: A density functional theory investigation.* The Journal of Physical Chemistry A, 2002. **106**(46): p. 11248-11253.

11.   Hicks, L.D., A.J. Fry, and V.C. Kurzweil, *Ab initio computation of electron affinities of substituted benzalacetophenones (chalcones): a new approach to substituent effects in organic electrochemistry.* Electrochimica Acta, 2004. **50**(4): p. 1039-1047.

12.   Namazian, M., S. Siahrostami, and M.L. Coote, *Electron affinity and redox potential of tetrafluoro-p-benzoquinone: A theoretical study.* Journal of Fluorine Chemistry, 2008. **129**(3): p. 222-225.

13.   Lu, J., et al., *DFT study of ionization potentials and electron affinities of formamide and its methylation derivatives.* Russian Journal of Physical Chemistry A, 2011. **85**(8): p. 1384-1389.

14.   Cooper, J.K., C.D. Grant, and J.Z. Zhang, *Ab initio calculation of ionization potential and electron affinity of six common explosive compounds.* Reports in Theoretical Chemistry, 2012. **1**: p. 11-19.

15.   Heßelmann, A., *Ionization energies and electron affinities from a random-phase-approximation many-body Green's-function method including exchange interactions.* Physical Review A, 2017. **95**(6): p. 062513.

16.   Zlatkis, A., et al., *Constant current linearization for determination of electron capture mechanisms.* Analytical Chemistry, 1983. **55**(9): p. 1596-1599.

17.   Pluharova, E., et al., *Transforming anion instability into stability: contrasting photoionization of three protonation forms of the phosphate ion upon moving into water.* The Journal of Physical Chemistry B, 2012. **116**(44): p. 13254-13264.

18.   Curtiss, L.A., P.C. Redfern, and K. Raghavachari, *Gaussian-4 theory using reduced order perturbation theory.* The Journal of chemical physics, 2007. **127**(12): p. 124105.

19.   Baboul, A.G., et al., *Gaussian-3 theory using density functional geometries and zero-point energies.* The Journal of chemical physics, 1999. **110**(16): p. 7650-7657.

20.   Ochterski, J.W., G.A. Petersson, and J.A. Montgomery Jr, *A complete basis set model chemistry. V. Extensions to six or more heavy atoms.* The Journal of chemical physics, 1996. **104**(7): p. 2598-2619.

21.   Montgomery Jr, J.A., et al., *A complete basis set model chemistry. VII. Use of the minimum population localization method.* The Journal of chemical physics, 2000. **112**(15): p. 6532-6542.

22.   Becke, A., *Density-functional thermochemistry. III. The role of exact exchange (1993) J.* Chem. Phys. **98**: p. 5648.

23.   Yanai, T., D.P. Tew, and N.C. Handy, *A new hybrid exchange–correlation functional using the Coulomb-attenuating method (CAM-B3LYP).* Chemical Physics Letters, 2004. **393**(1-3): p. 51-57.

24.   Iikura, H., et al., *A long-range correction scheme for generalized-gradient-approximation exchange functionals.* The Journal of chemical physics, 2001. **115**(8): p. 3540-3544.

25.   Boese, A.D. and J.M. Martin, *Development of density functionals for thermochemical kinetics.* The Journal of chemical physics, 2004. **121**(8): p. 3405-3416.

26.   Grimme, S., *Semiempirical GGA-type density functional constructed with a long-range dispersion correction.* Journal of computational chemistry, 2006. **27**(15): p. 1787-1799.

27.   Staroverov, V.N., et al., *Comparative assessment of a new nonempirical density functional: Molecules and hydrogen-bonded complexes.* The Journal of chemical physics, 2003. **119**(23): p. 12129-12137.

28.   Peverati, R. and D.G. Truhlar, *Improving the accuracy of hybrid meta-GGA density functionals by range separation.* The Journal of Physical Chemistry Letters, 2011. **2**(21): p. 2810-2817.

29.   Rajchel, Ł., et al., *A density functional theory approach to noncovalent interactions via interacting monomer densities.* Physical Chemistry Chemical Physics, 2010. **12**(44): p. 14686-14692.

30.   Zhao, Y. and D.G. Truhlar, *The M06 suite of density functionals for main group thermochemistry, thermochemical kinetics, noncovalent interactions, excited states, and transition elements: two*

new functionals and systematic testing of four M06-class functionals and 12 other functionals. Theoretical chemistry accounts, 2008. **120**(1): p. 215-241.

31. Zhao, Y., N.E. Schultz, and D.G. Truhlar, *Design of density functionals by combining the method of constraint satisfaction with parametrization for thermochemistry, thermochemical kinetics, and noncovalent interactions.* Journal of chemical theory and computation, 2006. **2**(2): p. 364-382.

32. Chakraborty, A., et al., *Combined valence bond-molecular mechanics potential-energy surface and direct dynamics study of rate constants and kinetic isotope effects for the H+ C 2 H 6 reaction.* The Journal of chemical physics, 2006. **124**(4): p. 044315.

33. Walker, M., et al., *Performance of M06, M06-2X, and M06-HF density functionals for conformationally flexible anionic clusters: M06 functionals perform better than B3LYP for a model system with dispersion and ionic hydrogen-bonding interactions.* The Journal of Physical Chemistry A, 2013. **117**(47): p. 12590-12600.

34. Peverati, R. and D.G. Truhlar, *Screened-exchange density functionals with broad accuracy for chemistry and solid-state physics.* Physical Chemistry Chemical Physics, 2012. **14**(47): p. 16187-16191.

35. Gaussian09, R.A., *1, mj frisch, gw trucks, hb schlegel, ge scuseria, ma robb, jr cheeseman, g. Scalmani, v. Barone, b. Mennucci, ga petersson et al., gaussian.* Inc., Wallingford CT, 2009. **121**: p. 150-166.

36. Mallard, W. and P. Linstrom, *National Institute of Standards and Technology (http://webbook. nist. gov): Gaithersburg, MD, 2012.* There is no corresponding record for this reference.[Google Scholar].

37. Barbas, R., et al., *Sildenafil–resorcinol cocrystal: XRPD structure and DFT calculations.* Crystals, 2020. **10**(12): p. 1126.

38. Yang, Y., et al., *A theoretical study on the proton affinity of sulfur ylides.* New Journal of Chemistry, 2022. **46**(17): p. 7910-7921.

39. Stephens, P.J., F.J. Devlin, and J.J. Pan, *The determination of the absolute configurations of chiral molecules using vibrational circular dichroism (VCD) spectroscopy.* Chirality: The Pharmacological, Biological, and Chemical Consequences of Molecular Asymmetry, 2008. **20**(5): p. 643-663.

40. Mardirossian, N. and M. Head-Gordon, *ωB97X-V: A 10-parameter, range-separated hybrid, generalized gradient approximation density functional with nonlocal correlation, designed by a survival-of-the-fittest strategy.* Physical Chemistry Chemical Physics, 2014. **16**(21): p. 9904-9924.

Theoretical calculation of the adiabatic electron affinities of the monosubstituted benzaldehyde derivatives

8   J. F. Lu, Y. F. Wu, Z. Y. Yu, X. J. Lin. "DFT study of ionization potentials and electron affinities of formamide and its methylation derivatives", Russian Journal of Physical Chemistry A, 2011
Crossref

54 mots — 1 %

9   Zaki S. Safi, Salama Omar. "Proton affinity and molecular basicity of m - and p -substituted benzamides in gas phase and in solution: A theoretical study", Chemical Physics Letters, 2014
Crossref

39 mots — 1 %

10   Zaki S. Safi, Nuha Wazzan. " Benchmark calculations of proton affinity and gas‗phase basicity using multilevel (and), and computational methods of para‗substituted benzaldehyde compounds ", Journal of Computational Chemistry, 2021
Crossref

30 mots — < 1 %

11   Koichi Kato, Yasuro Shinohara, Tomoki Nakayoshi, Eiji Kurimoto, Akifumi Oda, Yoshinobu Ishikawa. "Computational quantitation of the aldehyde forms of aldohexoses and disaccharides composed of d-glucose: predictions of their reactivities in the Maillard reaction", Computational and Theoretical Chemistry, 2022
Crossref

26 mots — < 1 %

12   scholars.unh.edu
Internet

25 mots — < 1 %

13   sro.sussex.ac.uk
Internet

24 mots — < 1 %

14   Jinfeng Lu, Songling Zhu, Zhengyu Zhou, Qunyan Wu, Gang Zhao. "DFT calculations of the

20 mots — < 1 %

ionization potentials and electron affinities of serinamide",
International Journal of Quantum Chemistry, 2006
Crossref

15   Ping Li, Yuxiang Bu, Hongqi Ai. "Theoretical   19 mots — < 1 %
      Determinations of Ionization Potential and
      Electron Affinity of Glycinamide Using Density Functional
      Theory", The Journal of Physical Chemistry A, 2004
      Crossref

16   cyberleninka.org   19 mots — < 1 %
      Internet

17   www.dovepress.com   17 mots — < 1 %
      Internet

18   lib.ugent.be   16 mots — < 1 %
      Internet

19   orbi.umons.ac.be   16 mots — < 1 %
      Internet

20   Mwadham M. Kabanda, Indra Bahadur.   15 mots — < 1 %
      "Hydrogen bonding between 1-ethyl-3-methyl-
      imidazolium dicyanamide ionic liquid and selected co-solvents
      with varying polarity: A DFT study", Journal of Molecular
      Liquids, 2022
      Crossref

21   Sivaprakasam Prasanna. "Glycogen synthase   15 mots — < 1 %
      kinase-3 inhibition by 3-anilino-4-
      phenylmaleimides: insights from 3D-QSAR and docking",
      Journal of Computer-Aided Molecular Design, 02/2009
      Crossref

22   www.koreascience.kr   15 mots — < 1 %
      Internet

23 Rifai, Ahmad, Sophie Bourcier, Farouk Jaber, and Guy Bouchoux. "Structures and dissociation mechanisms of protonated and electron ionized methamidophos", International Journal of Mass Spectrometry, 2013.
Crossref

14 mots — < 1 %

24 docksci.com
Internet

14 mots — < 1 %

25 moam.info
Internet

14 mots — < 1 %

26 naukarus.com
Internet

14 mots — < 1 %

27 Jiande Gu, Jerzy Leszczynski, Henry F. Schaefer. "Interactions of Electrons with Bare and Hydrated Biomolecules: From Nucleic Acid Bases to DNA Segments", Chemical Reviews, 2012
Crossref

13 mots — < 1 %

28 core.ac.uk
Internet

13 mots — < 1 %

29 dalspace.library.dal.ca
Internet

13 mots — < 1 %

30 Espinosa-Garcia, J., and F. J. Olivares del Valle. "New theoretical value of the enthalpy of formation of the hydroxymethyl radical", The Journal of Physical Chemistry, 1993.
Crossref

12 mots — < 1 %

31 digitalcommons.wayne.edu
Internet

12 mots — < 1 %

32 www.tru.ca
    Internet   12 mots — < 1 %

33 Emel'yanenko, Vladimir N., Sergey P. Verevkin,   11 mots — < 1 %
    Andreas Heintz, Jo-Anne Corfield, Alexey Deyko,
    Kevin R. J. Lovelock, Peter Licence, and Robert G. Jones.
    "Pyrrolidinium-Based Ionic Liquids. 1-Butyl-1-methyl
    Pyrrolidinium Dicyanoamide: Thermochemical Measurement,
    Mass Spectrometry, and ab Initio Calculations", The Journal of
    Physical Chemistry B, 2008.
    Crossref

34 Caminati, W.. "Molecular beam Fourier transform   10 mots — < 1 %
    microwave spectrum of the dimethylether-xenon
    complex: tunnelling splitting and ^1^3^1Xe quadrupole
    coupling constants", Chemical Physics Letters, 20040701
    Crossref

35 lab409.chem.ccu.edu.tw
    Internet   10 mots — < 1 %

36 mediatum.ub.tum.de
    Internet   10 mots — < 1 %

37 vdoc.pub
    Internet   10 mots — < 1 %

38 Carteret, C.. "An ab initio and DFT study of   9 mots — < 1 %
    structure and vibrational spectra of disiloxane
    H"3SiOSiH"3 conformers", Spectrochimica Acta Part A:
    Molecular and Biomolecular Spectroscopy, 200708
    Crossref

39 Dale E Wheeler, Nicholas W Baetz, Grant N Holder,   9 mots — < 1 %
    Scott T Hill, Steven Milos, Kraig A Luczak. "Cp*Ru+

complexes of benzylideneaniline and salicylideneaniline",
Inorganica Chimica Acta, 2002
Crossref

40   Jiří Šturala, Soňa Boháčová, Josef Chudoba, Radka
      Metelková, Radek Cibulka. "Electron-Deficient
      Heteroarenium Salts: An Organocatalytic Tool for Activation of
      Hydrogen Peroxide in Oxidations", The Journal of Organic
      Chemistry, 2015
      Crossref
                                                          9 mots — < 1 %

41   Lin, L.. "QSAR analysis of a series of 2-
      aryl(heteroaryl)-2,5-dihydropyrazolo[4,3-c]quinolin-
      3-(3H)-ones using piecewise hyper-sphere modeling by particle
      swarm optimization", Analytica Chimica Acta, 20051103
      Crossref
                                                          9 mots — < 1 %

42   Sein, L.T.. "Calculation of Hammett Equation
      parameters for some N,N'-bis (substituted-
      phenyl)-1,4-quinonediimines by density functional theory",
      Journal of Molecular Structure, 20110810
      Crossref
                                                          9 mots — < 1 %

43   Yu Takano, K. N. Houk. "Benchmarking the
      Conductor-like Polarizable Continuum Model
      (CPCM) for Aqueous Solvation Free Energies of Neutral and
      Ionic Organic Molecules", Journal of Chemical Theory and
      Computation, 2005
      Crossref
                                                          9 mots — < 1 %

44   repository.lib.ncsu.edu
      Internet
                                                          9 mots — < 1 %

45   ris.utwente.nl
      Internet
                                                          9 mots — < 1 %

46 Daniely V. V. Cardoso, Leonardo A. Cunha, Rene F. K. Spada, Corey A. Petty et al. " Thermochemical and Kinetics of CH SH + H Reactions: The Sensitivity of Coupling the Low and High-Level Methodologies ", The Journal of Physical Chemistry A, 2017
Crossref

8 mots — < 1 %

47 Dwarika Prasad, Rahul Singh, Zaki Safi, Nuha Wazzan, Lei Guo. "De-scaling, experimental, DFT, and MD-simulation studies of unwanted growing plant as natural corrosion inhibitor for SS-410 in acid medium", Colloids and Surfaces A: Physicochemical and Engineering Aspects, 2022
Crossref

8 mots — < 1 %

48 Gabriel da Silva, Eric M. Kennedy, Bogdan Z. Dlugogorski. "Ab Initio Study of Bonding between Nucleophilic Species and the Nitroso Group", The Journal of Physical Chemistry A, 2007
Crossref

8 mots — < 1 %

49 Ivan A. Konstantinov, Linda J. Broadbelt. "Reaction free energies in organic solvents: comparing different quantum mechanical methods", Molecular Simulation, 2010
Crossref

8 mots — < 1 %

50 Kainat Atiq, Riaz Hussain, Muhammad Adnan, Muhammad Usman Khan et al. "Investigating the Role of Novel Benzotrithiophene-Based Bat-Shaped Non-Fullerene Acceptors for High Performance Organic Solar Cells", Journal of Computational Biophysics and Chemistry, 2022
Crossref

8 mots — < 1 %

51 Kaining Duanmu, Joachim Friedrich, Donald G. Truhlar. "Thermodynamics of Metal Nanoparticles: Energies and Enthalpies of Formation of Magnesium Clusters

8 mots — < 1 %

and Nanoparticles as Large as 1.3 nm", The Journal of Physical Chemistry C, 2016
Crossref

52   Rachid Hsissou, Fouad Benhiba, Meriam El Aboubi, Said Abbout et al. "Synthesis and performance of two ecofriendly epoxy resins as a highly efficient corrosion inhibition for carbon steel in 1M HCl solution: DFT, RDF, FFV and MD approaches", Chemical Physics Letters, 2022   8 mots — < 1 %
Crossref

53   Rajeev S. Assary, Larry A. Curtiss. "Theoretical Study of 1,2-Hydride Shift Associated with the Isomerization of Glyceraldehyde to Dihydroxy Acetone by Lewis Acid Active Site Models", The Journal of Physical Chemistry A, 2011   8 mots — < 1 %
Crossref

54   Saha, Soumen, and G. Narahari Sastry. "Cooperative or Anticooperative: How Non-covalent Interactions Influence Each Other", The Journal of Physical Chemistry B   8 mots — < 1 %
Crossref

55   Xingzong Dong, Guangye Liu, Zhaoan Chen, Quan Zhang, Yunpeng Xu, Zhongmin Liu. "Activated carbon supported nitrogen-containing diheterocycle mercury-free catalyst for acetylene hydrochlorination", Molecular Catalysis, 2022   8 mots — < 1 %
Crossref

56   authors.library.caltech.edu   8 mots — < 1 %
Internet

57   cbc-wb01x.chemistry.ohio-state.edu   8 mots — < 1 %
Internet

| 58 | dspace.utlib.ee
Internet | 8 mots — < 1 % |

| 59 | eartharxiv.org
Internet | 8 mots — < 1 % |

| 60 | en.wikipedia.org
Internet | 8 mots — < 1 % |

| 61 | espace.cdu.edu.au
Internet | 8 mots — < 1 % |

| 62 | scholar.lib.vt.edu
Internet | 8 mots — < 1 % |

| 63 | www.qtp.ufl.edu
Internet | 8 mots — < 1 % |

| 64 | Jacob Schmidt, Steven R. Kass. "Zwitterion vs Neutral Structures of Amino Acids Stabilized by a Negatively Charged Site: Infrared Photodissociation and Computations of Proline–Chloride Anion", The Journal of Physical Chemistry A, 2013
Crossref | 7 mots — < 1 % |

| 65 | Jong-Won Song. "An improved long-range corrected hybrid exchange-correlation functional including a short-range Gaussian attenuation (LCgau-BOP)", The Journal of Chemical Physics, 2007
Crossref | 7 mots — < 1 % |

| 66 | Larry A. Curtiss. "Theoretical Methods for Computing Enthalpies of Formation of Gaseous Compounds", Reviews in Computational Chemistry, 01/01/2000
Crossref | 7 mots — < 1 % |

67 Mariela M. Nolasco, Catarina F. Araujo, Pedro D. Vaz, Ana M. Amado, Paulo Ribeiro-Claro. "Vibrational Dynamics of Crystalline 4-Phenylbenzaldehyde from INS Spectra and Periodic DFT Calculations", Molecules, 2020
Crossref

7 mots — < 1 %

68 Michiel J. van Setten, Fabio Caruso, Sahar Sharifzadeh, Xinguo Ren et al. " 100: Benchmarking for Molecular Systems ", Journal of Chemical Theory and Computation, 2015
Crossref

7 mots — < 1 %

69 Jalbout, A.. "Gaussian-based computations in molecular science", Journal of Molecular Structure: THEOCHEM, 20040223
Crossref

6 mots — < 1 %

70 Jason Cooper, Jin Zhang, Christian Grant. "Ab initio calculation of ionization potential and electron affinity of six common explosive compounds", Reports in Theoretical Chemistry, 2012
Crossref

6 mots — < 1 %

71 Qiu, Yong-Qing, Zhuo Li, Na-Na Ma, Shi-Ling Sun, Meng-Ying Zhang, and Peng-Jun Liu. "Third-order nonlinear optical properties of molecules containing aromatic diimides: Effects of the aromatic core size and a redox-switchable modification", Journal of Molecular Graphics and Modelling, 2013.
Crossref

6 mots — < 1 %